DOI: 10.1002/zaac.200900482

Halogenomercury Salts of Sterically Crowded Triazenides – Convenient Starting Materials for Redox-Transmetallation Reactions

Sven-Oliver Hauber,[a] Jang Woo Seo,[a] and Mark Niemeyer*[a]

Keywords: Magnesium; Mercury; Redox transmetallation; Triazenide ligands; Ytterbium

Abstract. Diaryl-substituted triazenides Ar(Ar')N_3HgX [Ar/Ar' = Dmp/Mph, X = Cl (**2a**), Br (**3a**), I (**4a**); Ar/Ar' = Dmp/Tph, X = Cl (**2b**), I (**4b**) with Mph = 2-MesC_6H_4, Mes = 2,4,6-$Me_3C_6H_2$, Tph = 2',4',6'-triisopropylbiphenyl-2-yl and Dmp = 2,6-$Mes_2C_6H_3$] were synthesized by salt-metathesis reactions in ethyl ether from the readily available starting materials Ar(Ar')N_3Li and HgX_2. These compounds may be used for redox-transmetallation reactions with rare-earth or alkaline earth metals. Thus, reaction of **4b** or **2b** with magnesium or ytterbium in tetrahydrofuran afforded the triazenides Dmp(Tph)N_3MX(thf) (**5b**: M = Mg, X = I; **6b**: M = Yb, X = Cl) in good yield. All new compounds were characterized by melting point, ^1H and ^{13}C NMR spectroscopy and for selected species by IR spectroscopy or mass spectrometry. In addition, the solid-state structures of triazenides **2a**, **2b**, **3a**, **4b**, **5b** and **6b** were investigated by single-crystal X-ray diffraction.

Introduction

The design and development of alternative ligand systems, which are able to stabilize monomeric metal complexes while provoking novel reactivity, remains one of the most intensively studied areas of organometallic chemistry [1]. Exploration of this field is driven by the potential use of these complexes in catalysis and organic synthesis. Examples of monoanionic chelating N-donor ligands that have received much recent attention include the β-diketiminate [2] and the amidinate [3] ligand systems. Much less attention has been given to the closely related triazenides [4]. We recently succeeded in the preparation of derivatives of aryl-substituted, sterically crowded triazenido ligands that are bulky enough to prevent undesirable ligand redistribution reactions [5–8]. These ligands were used to stabilize the first examples of structurally characterized aryl compounds of the heavier alkaline earth metals calcium, strontium, and barium [5] and unsolvated pentafluorophenyl organyls of the divalent lanthanides ytterbium and europium [9]. We also examined the unusual "inverse" aggregation behavior of alkali metal triazenides in their solid-state structures that can be traced back to a different degree of metal···π-arene interactions to pending aromatic substituents [6]. A series of homologous potassium and thallium complexes crystallizes in isomorphous cells and consists of the first examples of isostructural molecular species reported for these elements [10].

In this paper, we describe the synthesis and characterization of several halogenomercury triazenides. These compounds are useful transfer reagents for redox transmetalation reactions with electropositive elements such as rare-earth or alkaline earth metals. As a proof of principle the reaction of halogenomercury triazenides with magnesium or ytterbium metal was examined.

Results and Discussion

Synthesis

Diaryl-substituted halogenomercury triazenides Ar(Ar')N_3HgX [Ar/Ar' = Dmp/Mph, X = Cl (**2a**), Br (**3a**), I (**4a**); Ar/Ar' = Dmp/Tph, X = Cl (**2b**), I (**4b**) with Mph = 2-MesC_6H_4, Mes = 2,4,6-$Me_3C_6H_2$, Tph = 2',4',6'-triisopropylbiphenyl-2-yl and Dmp = 2,6-$Mes_2C_6H_3$] were synthesized by salt-metathesis reactions in ethyl ether from the readily available starting materials Ar(Ar')N_3Li and HgX_2 (Scheme 1). After crystallization from *n*-heptane, the yellow compounds were isolated in moderate or good yields (56–90 %).

The triazenides are air-stable in the solid-state for days and decompose with evolution of gas in the range 152–194 °C. Since the used triazenide ligands show an asymmetric substitution pattern, the existence of isomers with different Hg–N coordination modes, such as η^1-*N*NNAr(Ar'), η^1-NN*N*Ar(Ar') or η^2-*N*N*N*Ar(Ar'), should be possible in principle. However, in the ^1H and ^{13}C NMR spectra only one set of signals is observed for each compound, which indicates either the absence of different isomers or, more probably, fast exchange on the NMR time scale between them. In the IR spectra the asymmetric *N*–*N*=N and N–*N*=*N* vibration modes ν_{as} of the deprotonated triazenide ligand appear as medium or strong bands in the range 1163–1169 cm^{-1} and 1405–1423 cm^{-1}, which indi-

---

* PD Dr. M. Niemeyer
E-Mail: mn@lanth.de
[a] Institut für Anorganische und Analytische Chemie
Johannes Gutenberg-Universität Mainz
Duesbergweg 10–14
55128 Mainz, Germany

Supporting information for this article is available on the WWW under **http://dx.doi.org/10.1002/zaac.200900482** or from the author.

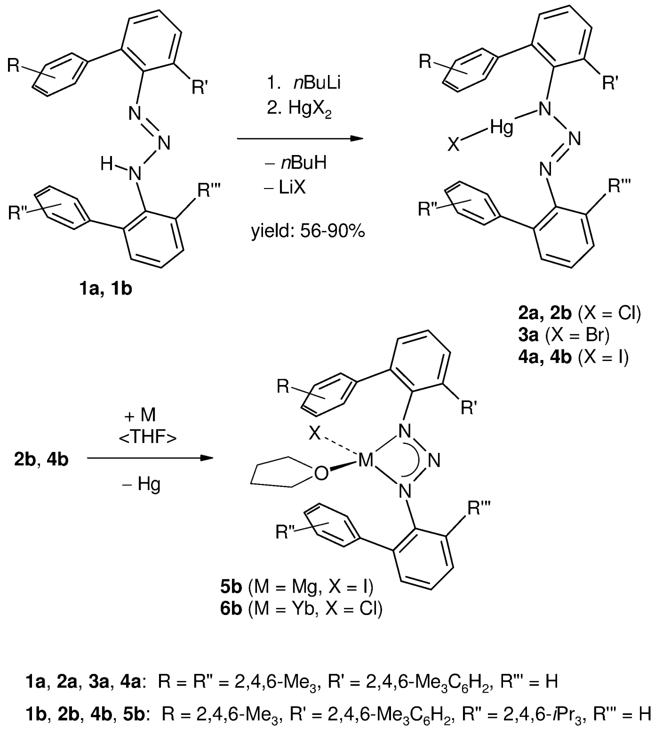

Scheme 1. Synthesis of compounds **2a**–**6d**.

cates a mainly localized π-electron system [4a]. These values are similar to the corresponding vibrations in the protonated ligands [Dmp(Tph)N_3H (**1a**): 1143/1473 cm^{-1}; Dmp(Mph)N_3H (**1b**): 1169/1472 cm^{-1}], whereas strong absorptions in the range 1230–1295 cm^{-1} are indicative for the triazenides acting as chelating ligands [5, 6, 9, 10].

In order to test the propensity of the halogenomercury triazenides to act as transfer reagents for redox transmetalation reactions with rare-earth or alkaline earth metals, we examined the reaction of **4b** with magnesium turnings in tetrahydrofuran as solvent. After an induction period of several hours, deposition of finely divided mercury was observed and stirring was continued for a total of 3 days. Removal of solvent and crystallization from *n*-heptane afforded the deep yellow transmetalation product Dmp(Tph)N_3MgI(thf) (**5b**) in 68 % yield. A similar reaction between the chloromercury triazenide **2b** and ytterbium chips gave the heteroleptic complex Dmp(Tph)N_3YbCl(thf) (**6b**) in 77 % yield. Although this composition together with the oxidation state of the metal was confirmed by single-crystal X-ray diffraction (see below) we could not obtain a reasonable NMR spectrum due to some paramagnetic impurities that proved difficult to separate by crystallization.

Solid-State Structures

Compounds **2a**, **2b**, **3a**, **4b**, **5b**, and **6b** were characterized by X-ray crystallography and the molecular structures of **2a**, **4b**, **5b**, and **6b** are shown in Figure 1, Figure 2, Figure 3, and Figure 4. Further molecular plots are provided in the Supporting Information. Pertinent bond parameters are summarized in Table 1 and Figure 3 and Figure 4.

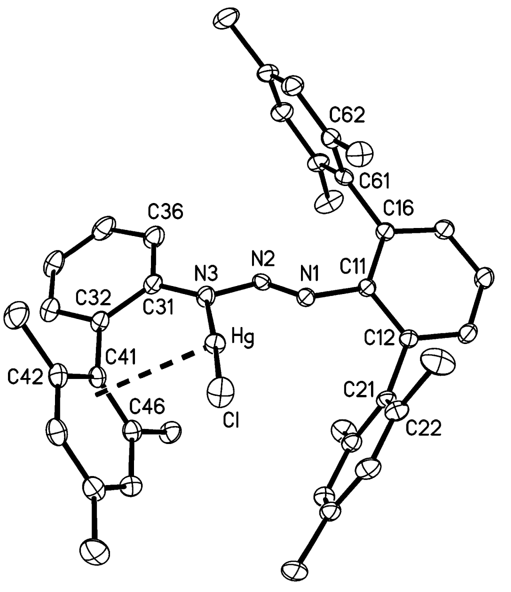

Figure 1. Molecular structure of **2a**, showing thermal ellipsoids at the 30 % probability level and the numbering scheme. Hydrogen atoms and minor parts of disordered groups have been omitted for clarity.

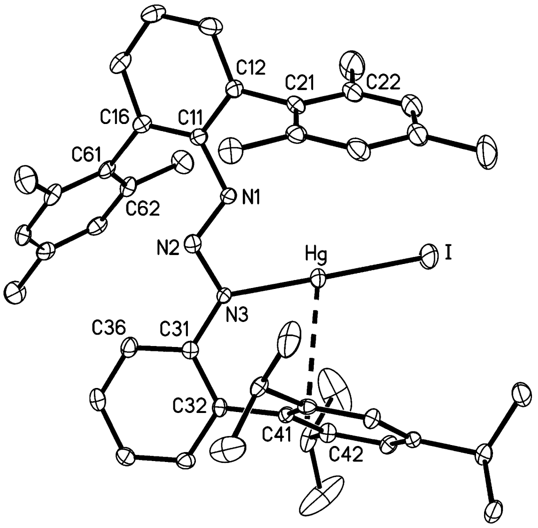

Figure 2. Molecular structure of **4b**, showing thermal ellipsoids at the 30 % probability level and the numbering scheme. Hydrogen atoms and minor parts of disordered groups have been omitted for clarity.

The Dmp- and Mph-substituted halogenomercury triazenides **2a** and **3a** crystallize in isomorphous cells in the space group $P\bar{1}$. Attempts to grow X-ray quality crystals of the iodo derivative **4a** were unsuccessful. Structurally characterized mercury triazenides have been limited so far to several unsolvated [11] and solvated bis(diaryltriazenido) species [12], a mercury nitrate [13] and two heterobimetallic complexes [14]. Very recently, the structural characterization of a donor-stabilized mercury chloride was reported [15]. For **2a** and **3a** the size of the η^1-bonded triazenide ligands enforces the formation of

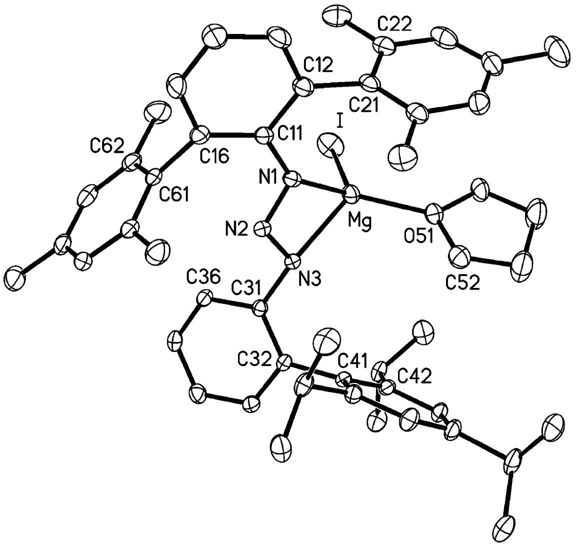

Figure 3. Molecular structure of **5b**, showing thermal ellipsoids at the 30 % probability level and the numbering scheme. Hydrogen atoms have been omitted for clarity. Selected bond lengths /Å, angles /deg and torsion angles /deg: Mg–N1 = 2.074(3), Mg–N3 = 2.112(3), Mg···N2 = 2.537(3), Mg–I = 2.6424(13), Mg–O51 = 1.975(2), N1–N2 = 1.319(3), N2–N3 = 1.314(3), O51–Mg–I = 111.87(8), N2···Mg–I = 117.61(7), N2···Mg–O51 = 129.39(10), N1–Mg–N3 = 61.92(9), N1–N2–N3 = 109.8(2), N2–N1–C11–C16 = –17.2(4), N2–N3–C31–C36 = 45.6(4).

Table 1. Selected bond lengths /Å, angles /deg and torsion angles /deg for the triazenes Ar(Ar')N_3Hg*X*.

	2a	**3a**	**2b**	**4b**
Ar/Ar'/*X*	Dmp/Mph/Cl	Dmp/Mph/Br	Dmp/Tph/Cl	Dmp/Tph/I
M–*X*	2.2847(13)	2.404(2)	2.2880(15)	2.5543(6)
M–N3	2.090(3)	2.153(12)	2.084(4)	2.100(4)
M···N1	2.638(3)	2.641(11)	2.737(4)	2.674(4)
M···N2	2.856(3)	2.862(11)	2.895(4)	2.864(4)
N1–N2	1.253(4)	1.237(15)	1.267(5)	1.289(6)
N2–N3	1.335(4)	1.321(16)	1.328(5)	1.322(6)
M···C41	2.972(4)	2.975(14)	2.917(5)	3.049(5)
M···C42	3.255(4)	3.297(15)	3.221(5)	3.425(6)
M···C46	3.141(4)	3.125(15)	3.172(5)	3.245(5)
M···*X*3	2.946	2.950	2.920	3.068
X–*M*–N3	174.64(9)	173.2(3)	175.71(11)	175.58(12)
N2–N1–C11–C16	50.4(5)	51.1(1.7)	–42.0(6)	–36.2(8)
N2–N3–C31–C36	–28.8(5)	–29(2)	13.7(6)	18.3(7)

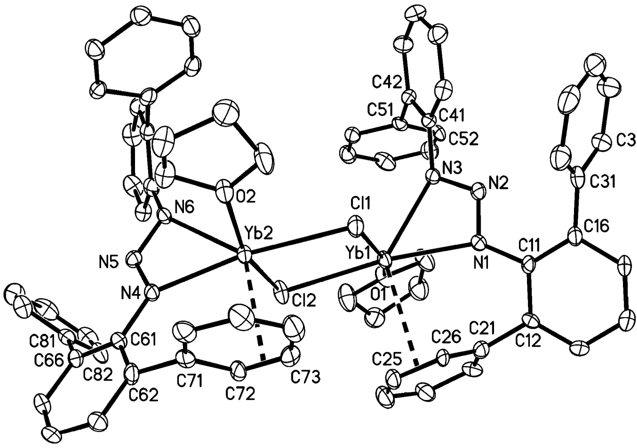

Figure 4. Molecular structure of dimeric **6b**, showing thermal ellipsoids at the 30 % probability level and the numbering scheme. Hydrogen, methyl carbon and *isopropyl* carbon atoms have been omitted for clarity. Selected bond lengths /Å, angles /deg and torsion angles /deg: Yb1–N1 = 2.439(6), Yb1–N3 = 2.530(6), Yb2–N4 = 2.440(6), Yb2–N6 = 2.547(6), Yb1–Cl1 = 2.751(2), Yb1–Cl2 = 2.782(2), Yb2–Cl1 = 2.783(2), Yb2–Cl2 = 2.732(2), Yb1–O1 = 2.390(6), Yb2–O2 = 2.387(6), Yb1···C26 = 3.032(8), Yb1···C25 = 3.085(9), Yb2···C72 = 3.023(8), Yb2···C73 = 3.198(8), N1–Yb1–N3 = 51.5(2), N4–Yb2–N6 = 51.52(19), Cl1–Yb1–Cl2 = 80.89(6), Cl1–Yb2–Cl2 = 81.20(6), Yb1–Cl1–Yb2 = 98.59(7), Yb2–Cl2–Yb1 = 99.08(7), N2–N1–C11–C16 = 14.3(12), N2–N3–C41–C46 = –47.0(9), N5–N4–C61–C66 = 12.1(11), N5–N6–C91–C96 = –44.1(9).

strictly monomeric compounds in which the metal atoms show a linear coordination by the Mph-bonded nitrogen atom N3 and one halogen atom, respectively. The Hg–N3 distances of 2.090(3) Å (**2a**) and 2.153(12) Å (**3a**) are similar or slightly longer than the corresponding distances in three structurally characterized homoleptic mercury triazenides [2.060(5)–2.077(4) Å] [11], a triazenidomercury nitrate [2.101(8) Å] [13] and a donor-stabilized triazenidomercury chloride [2.075(4) Å] [15]. Much longer distances are observed to the Dmp-bonded nitrogen atom N1 and the central nitrogen atom N2 with values > 2.63 Å and > 2.85 Å, respectively. Within the triazenido ligand cores, the rather different N1–N2 and N2–N3 distances of 1.253(4)/1.335(4) Å (**2a**) and 1.237(15)/1.321(16) Å (**3a**) are in agreement with the observed η^1-N-bonding mode. The different steric properties of the biphenyl- and *m*-terphenyl substituents give rise to a different conformation with respect to the central N_3 plane. The C_6H_4 ring of the biphenyl moiety adopts a roughly coplanar arrangement (N2–N3–C31–C36 –28.8(5) [**2a**], –29(2) [**3a**]), whereas the central C_6H_3 plane of the terphenyl substituent is significantly more tilted (N2–N1–C11–C16 50.4(5) [**2a**], 51.1(1.7) [**3a**]) to minimize repulsive interactions between N2 and one of the Mes rings (C61→C66). One interesting feature in the solid-state structures of **2a** and **3a** is the presence of an additional metal···η^3-π-arene contact to the (C41→C46) Mes ring of the flanking Mph group with relatively short Hg···C distances in the range 2.972(4)–3.255(4) Å (**2a**) or 2.975(14)–3.297(15) Å (**3a**) and corresponding Hg···centroid (X3) separations of 2.946 Å and 2.950 Å, respectively. The propensity of mercury to interact with aromatic groups is now well documented. Examples are packing complexes of mercury perfluoroaryls with arenes {e.g. $Hg_3(o\text{-}C_6F_4)_3$(arene) [16] or $Hg(C_6F_5)_2$(arene) [17]} and inter- or intramolecular contacts between mercury and arene rings of aryl substituents in organometallic [e.g. $Hg(CH_2Ph)_2$ [18a] or $HgDmp_2$ [18b]) or coordination compounds (e.g. weak intermolecular coordination in mercury triazenides: [11, 12]) with typical Hg···C distances in the range 3.15–3.50 Å. Considerably shorter mercury···arene interactions are observed in arene complexes of inorganic mercury salts $[Hg_2(O_2CCF_3)_4(\eta^2\text{-}C_6Me_6)_2]$ (2.56, 2.58 Å) [19a] or $Hg(arene)_2(M Cl_4)_2$] [*M* = Ga, Al; arene = C_6H_5Me, C_6H_5Et, 1,2-$C_6H_4Me_2$, 1,2,3-$C_6H_3Me_3$] (2.27–2.74 Å) [19b].

In contrast to isomorphous **2a** and **3a**, the Dmp- and Tph-substituted halogenomercury triazenides **2b** and **4b** crystallize in different cell settings in the space group $P\bar{1}$ and $P2_1/n$, respectively. Figure 2 shows the molecular structure of the iodo complex **4b**. The average Hg–N3 distances of 2.084(4) Å [**2b**] or 2.100(4) Å [**4b**] to the η^1-coordinate triazenide ligand are very close to the corresponding values in the previously discussed compounds. Additional metal···η^3-π-arene are observed to the Trip ring (C41→C46) of the flanking biaryl group. With Hg···C distances of 2.917(5)–3.221(5) Å and a Hg···centroid separation of 2.920 Å these secondary interactions are stronger for the chloro than for the iodo (3.049(5)–3.425(6) Å / 3.068 Å) derivative.

Because of the different steric properties of the Dmp and Tph substituents and inter-ligand repulsion the N2–N1–C11–C16 (–42.0(6) [**2b**], –36.2(8) [**4b**]) and N2–N3–C31–C36 (13.7(6) [**2b**], 18.3(7) [**4b**]) torsion angles differ by approx. 28° [**2b**] and 18° [**4b**]. Therefore, a different interaction of the π-system of the central NNN fragment with that of the substituted C_6H_4 rings is anticipated. As in the Dmp/Mph compounds, these conformational differences, together with steric factors, are probably responsible for the higher nucleophilicity of the biphenyl-substituted nitrogen atom N3. This explanation is supported by the observation of disordered mercury sites with minor site occupation factors in the range 0.017–0.039 for complexes **2a**, **3a** and **4b** that correspond to a Hg–η^1-N1 coordination mode with bonding to the terphenyl-substituted nitrogen atom (see Experimental Section and Supporting Information). For these compounds the difference of the N2–N1–C11–C16 and N2–N3–C31–C36 torsion angles is smaller than in complex **2b** which shows no disorder of the mercury atom.

In the triazenido magnesium iodide (**5b**) the magnesium atom has a very distorted tetrahedral coordination with angles in the range 61.92(9)–125.20(11)° by two nitrogen atoms N1 and N3 of a η^2-bonded triazenide ligand, a chlorine atom and the oxygen atom O51 of a THF molecule. In an alternative description that assigns only one coordination site (represented by the central nitrogen atom N2) to the small-bite triazenido ligand the metal atom shows a trigonal planar coordination with corresponding angles of 111.87(8)–129.39(10)°. With 1.319(3) Å and 1.314(3) Å the N–N distances are consistent with delocalized bonding. The coordination of the triazenide ligand is slightly asymmetric with Mg–N bond lengths of 2.074(3) Å and 2.112(3) Å. The average Mg–N distance of 2.093 Å is shorter than that of the six-coordinate magnesium triazenide $[Mg\{N_3Tol_2\}_2(thf)_2]$ (2.183 Å with Tol = 4-Me-phenyl) the currently only structurally characterized triazenide available for comparison [20]. Shorter Mg–N bonds but longer Mg–I and Mg–O distances are observed in the heteroleptic β-diketiminate $(Dip\text{-}nacnac)_2MgI(OEt_2)$ [Dip-nacnac = (Dip)NC(Me)C(H)C(Me)N(Dip) with Dip = 2,6-$i\mathrm{Pr}_2C_6H_3$] (Mg–N = 2.040(3) Å, Mg–I = 2.689(1) Å, Mg–O = 2.010(3) Å] [21] and a number of homoleptic magnesium amidinates $Mg\{RNC(R')NR\}_2$ (R = *t*Bu, R' = Ph, av. Mg–N = 2.042(2) Å [22a]; R = *i*Pr, R' = Dmp, av. Mg–N = 2.04(1) Å [22b]; R = Mes, R' = *t*Bu, av. Mg–N = 2.041(3) Å [22c]; R = Dip, R' = Tol, av. Mg–N = 2.058(2) Å [22d]). These differences reflect the lower donor ability of the triazenide relative to the amidinate and β-diketiminate ligands.

Triazenido ytterbium chloride (**6b**) crystallizes as a dimer, and its molecular structure is shown in Figure 4. In the dimeric units the metal atoms are bridged by chlorine atoms, therefore forming a central, almost planar Yb_2Cl_2 ring. The dimers have non-crystallographic symmetry close to C_2 with the twofold axis running perpendicular to the Yb_2Cl_2 core. However, the symmetry is broken by slight but significant conformational differences between the two halves and the presence of four additional co-crystallized toluene molecules that are located in solvent accessible cavities of the structure. Each ytterbium atom is bonded to two chlorine atoms, two nitrogen atoms of a η^2-bonded triazenide ligand and the oxygen atom of a THF molecule. If only one coordination site is assigned to the small-bite angle triazenido ligands, a distorted square-planar coordination results for both ytterbium atoms as can be judged by the angles N2/N5–Yb1/Yb2–Cl2/Cl1 and O1/O2–Yb1/Yb2–Cl1/Cl2 that are in the range 160.3–163.8°. An additional metal···η^2-π-arene contact to *ortho* and *meta* carbon atoms of a Mes ring of the flanking Dmp substituents with Yb···C distances of 3.023(8)–3.198(8) Å extends the coordination for each metal atom to tetragonal-pyramidal. The bonding of the triazenide ligands is slightly asymmetric with shorter and longer Yb–N bond lengths of 2.439(6)/2.440(6) Å and 2.530(6)/2.547(6) Å, respectively. The average Yb–N distance of 2.489 Å is longer than that of the heteroleptic ytterbium triazenide $[Yb\{N_3(Dmp)Tph\}C_6F_5]$ (2.445 Å) the currently only structurally characterized triazenide available for comparison [9]. Shorter M–N distances are observed in some tetracoordinate homoleptic ytterbium amidinates (2.38–2.39 Å) [23] and diketiminates (2.37–2.41 Å) [24] therefore reflecting the lower coordination number and the stronger donor character of the chelating N-donor ligands in these compounds. For **6b**, the average Yb–Cl and Yb–O bond lengths of 2.762(2) Å and 2.389(6) Å are in accordance with the presence of divalent metal atoms. Similar values are observed for the Yb^{II} complex $[Yb\{N(Dip)SiMe_3\}(\mu\text{-}Cl)(thf)_2]_2$ (av. Yb–Cl 2.72 Å, Yb–O 2.40 Å) [25], that features a pentacoordinate metal atom, whereas the corresponding distances for some structurally related Yb^{III} compounds such as $[Yb\{N(Ph)SiMe_3\}_2(\mu\text{-}Cl)(thf)]_2$ (av. Yb–Cl 2.67 Å, Yb–O 2.32 Å) [25], $[Yb\{N(SiMe_3)_2\}_2(\mu\text{-}Cl)(thf)]_2$ (av. Yb–Cl 2.68 Å, Yb–O 2.35 Å) [26a] or $[Yb\{N(t\mathrm{Bu})SiMe_2SiMe_2(t\mathrm{Bu})N\}(\mu\text{-}Cl)(thf)]_2$ (av. Yb–Cl 2.70 Å, Yb–O 2.31 Å) [26b] are considerably shorter, as one might expect.

Conclusions

Monomeric unsolvated triazenido mercury halides were synthesized and structurally characterized for the first time. We have shown that these compounds may be used for the preparation of triazenido magnesium and ytterbium halides. We anticipate a similar reactivity for redox-transmetallation reactions with other alkaline earth and rare-earth elements.

Experimental Section

General Remarks

All manipulations were performed by using standard Schlenk techniques in an inert atmosphere of purified argon and solvents freshly distilled from sodium wire or $LiAlH_4$. The triazenes Dmp(Mph)N_3H or Dmp(Tph)N_3H [5] were synthesized as described previously. NMR spectra were recorded in C_6D_6 with Bruker AM200, AC250 or AM400 instruments and referenced to solvent resonances. IR spectra were obtained in the range 4000–200 cm^{-1} with a Perkin–Elmer paragon 1000 PC (Nujol mulls) or a Nicolet 6700 FT-IR (reflection data) spectrometer. Mass spectra were recorded with a Varian MAT711 or Finnegan MAT95 instrument. Melting points were determined under argon atmosphere in sealed glass tubes. No elemental analysis data for compounds **2a**–**4b** could be obtained due to mercury contamination problems. Therefore, purity of these compounds was proven by combined NMR and mass spectrometry experiments.

Preparation of the Triazenido Mercury Halides

Chloro-{[[N'-2-(2',4',6'-trimethyl)biphenyl]-(N'''-2,4,6,2'',4'',6''-hexamethyl-1,1':3',1''-terphen-2'-yl)]triazenido-N'}mercury (2a): To a stirred solution of **1a** (1.10 g, 2 mmol) in ethyl ether (20 mL), which was cooled in an ice bath was added *n*-BuLi in *n*-hexane (0.80 mL, 2.5 M, 2 mmol) and stirring was continued for 30 min at the same temperature. $HgCl_2$ (0.54 g, 2.00 mmol) was afterwards added in one portion and the resulting mixture was stirred at ambient temperature for 4 h. The volatile materials were removed under reduced pressure and the remaining solid was extracted with *n*-heptane (20 mL). After separation of the precipitated lithium halide by centrifugation the filtrate was concentrated to incipient crystallization. Cooling in a –20 °C freezer afforded **2a** as yellow crystals. Yield: 0.88 g (1.12 mmol, 56 %); Mp: 165–167 °C. **^{1}H NMR** (250.1 MHz): δ = 1.60 (s, 6 H, *o*-CH_3, biphenyl), 2.11 (s, 12 H, *o*-CH_3, terphenyl), 2.24 (s, 3 H, *p*-CH_3, biphenyl), 2.26 (s, 6 H, *p*-CH_3, terphenyl), 6.76 (s, 2 H, *m*-Mes, biphenyl), 6.89 (s, 4 H, *m*-Mes, terphenyl), 6.71–7.11 (m, 7 H, various aryl-H). **^{13}C NMR** (62.9 MHz): δ = 20.2 (*o*-CH_3, biphenyl), 21.0 (*o*-CH_3, terphenyl), 21.2 (*p*-CH_3, terphenyl), 21.3 (*p*-CH_3, biphenyl), 120.2, 123.8, 126.4, 128.3, 128.7, 129.5, 129.8, 130.3 (aromatic *C*H), 128.8, 132.9, 135.1, 135.7, 136.6, 136.8, 137.5, 139.2, 143.5, 143.6 (aromatic *C*). **IR** (Nujol): 1716 w, 1699 w, 1611 m, 1557 w, 1436 w, 1418 w, 1316 m br, 1206 m, 1186 m, 1164 m br, 1098 m, 1030 m br, 982 m, 911 w, 847 s, 805 ms, 790 m, 761 s, 735 m, 691 m, 652 s, 597 s, 576 m, 514 s, 499 m, 463 m, 463 m, 443 m cm^{-1}. **EI-MS** (70eV, 430 K): *m*/*z* (%) 195.0 (32.6) $[MesC_6H_4^+]$, 313.2 (100) $[2,6\text{-}Mes_2C_6H_3\text{–}H^+]$, 341.2 (12.4) $[2,6\text{-}Mes_2C_6H_3N_2^+]$, 523.3 (3.1) $[(2,6\text{-}Mes_2C_6H_3)(C_6H_4Mes)NH^+]$, 787.3 (2.7) $[M^+]$.

Bromo-{[[N'-2-(2',4',6'-trimethyl)biphenyl]-(N'''-2,4,6,2'',4'',6''-hexamethyl-1,1':3',1''-terphen-2'-yl)]triazenido-N'}mercury (3a): The synthesis was accomplished in a similar manner to the preparation of **2a** with use of triazene (**1a**) (1.10 g, 2 mmol), *n*-BuLi in *n*-hexane (0.80 mL, 2.5 M, 2 mmol) and $HgBr_2$ (0.72 g, 2 mmol). Yield: 0.98 g (1.18 mmol, 59 %); Mp: 161–163 °C. **^{1}H NMR** (200.1 MHz): δ = 1.61 (s, 6 H, *o*-CH_3, biphenyl), 2.11 (s, 12 H, *o*-CH_3, terphenyl), 2.24 (s, 3 H, *p*-CH_3, biphenyl), 2.26 (s, 6 H, *p*-CH_3, terphenyl), 6.75 (s, 2 H, *m*-Mes, biphenyl), 6.89 (s, 4 H, *m*-Mes, terphenyl), 6.70–7.19 (m, 7 H, various aryl-H). **^{13}C NMR** (50.3 MHz): δ = 20.2 (*o*-CH_3, biphenyl), 21.0 (*o*-CH_3, terphenyl), 21.2 (*p*-CH_3, terphenyl), 21.3 (*p*-CH_3, biphenyl), 120.2, 123.8, 126.4, 128.3, 128.8, 129.5, 130.0, 130.3, (aromatic *C*H), 129.0, 133.1, 135.1, 135.1, 136.6, 136.8, 137.5, 139.0, 143.6 (aromatic *C*); one aromatic C signal could not be observed. **EI-MS** (70eV, 430 K): *m*/*z* (%) 195.1 (38.4) $[MesC_6H_4^+]$, 313.3 (100) $[2,6\text{-}Mes_2C_6H_3\text{–}H^+]$, 341.2 (15.1) $[2,6\text{-}Mes_2C_6H_3N_2^+]$, 523.4 (10.3) $[(2,6\text{-}Mes_2C_6H_3)(C_6H_4Mes)NH^+]$, 831.3 (2.4) $[M^+]$.

Iodo-{[[N'-2-(2',4',6'-trimethyl)biphenyl]-(N'''-2,4,6,2'',4'',6''-hexamethyl-1,1':3',1''-terphen-2'-yl)]triazenido-N'}mercury (4a): The synthesis was accomplished in a similar manner to the preparation of **2a** with use of triazene (**1a**) (1.10 g, 2 mmol), *n*-BuLi in *n*-hexane (0.80 mL, 2.5 M, 2 mmol) and HgI_2 (0.91 g, 2 mmol). Yield: 1.12 g (1.17 mmol, 58 %); Mp: 192–194 °C. **^{1}H NMR** (400.1 MHz): δ = 1.63 (s, 6 H, *o*-CH_3, biphenyl), 2.11 (s, 12 H, *o*-CH_3, terphenyl), 2.24 (s, 3 H, *p*-CH_3, biphenyl), 2.26 (s, 6 H, *p*-CH_3, terphenyl), 6.73 (s, 2 H, *m*-Mes, biphenyl), 6.88 (s, 4 H, *m*-Mes, terphenyl), 6.73–7.17 (m, 7 H, various aryl-H). **^{13}C NMR** (100.6 MHz): δ = 20.3 (*o*-CH_3, biphenyl), 21.0 (*o*-CH_3, terphenyl), 21.3 (*p*-CH_3, terphenyl), 21.5 (*p*-CH_3, biphenyl), 120.1, 123.8, 126.2, 128.2, 129.0, 129.2, 129.6, 130.3 (aromatic *C*H), 128.3, 133.6, 135.1, 135.8, 136.5, 136.8, 137.6, 138.8, 143.6, 143.9 (aromatic *C*). **IR** (Nujol): 1716 w, 1699 w, 1611 m, 1557 w, 1436 w, 1418 w, 1316 m br, 1205 m, 1169 m br, 1099 m, 1069 w, 1026 m br, 981 m, 846 s, 806 s, 789 m, 759 s, 734 m, 688 m, 651 s, 697 m, 572 w, 511 m, 496 m, 462 m, 438 m cm^{-1}. **EI-MS** (70eV, 420 K): *m*/*z* (%) 195.1 (45.4) $[MesC_6H_4^+]$, 313.2 (100) $[2,6\text{-}Mes_2C_6H_3\text{–}H^+]$, 341.2 (16.2) $[2,6\text{-}Mes_2C_6H_3N_2^+]$, 523.3 (8.2) $[(2,6\text{-}Mes_2C_6H_3)(C_6H_4Mes)NH^+]$, 897.2 (2.7).

Chloro-{[[N'-2-(2',4',6'-triisopropyl)biphenyl]-(N'''-2,4,6,2'',4'',6''-hexamethyl-1,1':3',1''-terphen-2'-yl)]triazenido-N'}mercury (2b): The synthesis was accomplished in a similar manner to the preparation of **2a** with use of triazene (**1b**) (1.27 g, 2.00 mmol), *n*-BuLi in *n*-hexane (0.80 mL, 2.5 M, 2 mmol) and $HgCl_2$ (0.59 g, 2.17 mmol). Yield: 1.46 g (1.68 mmol, 84 %); Mp: 173–175 °C (dec.). **^{1}H NMR** (400.1 MHz): δ = 0.87, 0.90 (2 × d, $^3J_{HH}$ = 6.7 Hz, 2 × 6 H, *o*-$CH(CH_3)_2$), 1.32 (d, $^3J_{HH}$ = 6.7 Hz, 6 H, *p*-$CH(CH_3)_2$), 2.11 (s, 12 H, *o*-CH_3), 2.24 (s, 6 H, *p*-CH_3), 2.47 (sep, $^3J_{HH}$ = 6.7 Hz, 2 H, *o*-$CH(CH_3)_2$), 2.86 (sep, $^3J_{HH}$ = 6.7 Hz, 1 H, *p*-$CH(CH_3)_2$), 6.69 (d, $^3J_{HH}$ = 8.2 Hz, 1 H, *6*-C_6H_4), 6.85 (t, $^3J_{HH}$ = 7.7 Hz, 1 H, *4*-C_6H_4), 6.88 (d, 1 H, *3*-C_6H_4), 6.90 (s, 4 H, *m*-Mes), 7.00 (m, 2 H, *m*-C_6H_3), 7.06 (m, 1 H, *p*-C_6H_3), 7.12 (t, 1 H, *5*-C_6H_4), 7.14 (s, 2 H, *m*-Trip). **^{13}C NMR** (100.6 MHz): δ = 21.0 (*o*-CH_3), 21.2 (*p*-CH_3), 24.1, 24.2 (*o*-$CH(CH_3)_2$), 24.7 (*p*-$CH(CH_3)_2$), 30.5 (*o*-$CH(CH_3)_2$), 34.8 (*p*-$CH(CH_3)_2$), 119.3 (6-C_6H_4), 122.9 (4-C_6H_4), 123.0 (*m*-Trip), 126.6 (p-C_6H_3), 128.6 (5-C_6H_4), 128.8 (*m*-Mes), 129.8 (m-C_6H_3), 131.2 (3-C_6H_4), 127.0, 131.3, 135.2, 135.4, 136.5, 137.7, 143.4, 144.2, 147.6, 151.1 (aromatic *C*).

Iodo-{[[N'-2-(2',4',6'-triisopropyl)biphenyl]-(N'''-2,4,6,2'',4'',6''-hexamethyl-1,1':3',1''-terphen-2'-yl)]triazenido-N'}mercury (4b): The synthesis was accomplished in a similar manner to the preparation of **2a** with use of triazene (**1b**) (0.83 g, 1.30 mmol), 0.52 mL of a 2.5 M *n*-BuLi solution in *n*-hexane (0.52 mL, 2.5 M, 1.3 mmol) and HgI_2 (0.70 g, 1.54 mmol). Yield: 1.14 g (1.18 mmol, 90 %); Mp: 152 °C (dec.). **^{1}H NMR** (250.1 MHz): δ = 0.91, 0.92 (2 × d, $^3J_{HH}$ = 6.8 Hz, 2 × 6 H, *o*-$CH(CH_3)_2$), 1.31 (d, $^3J_{HH}$ = 6.8 Hz, 6 H, *p*-$CH(CH_3)_2$), 2.21 (s, 12 H, *o*-CH_3), 2.22 (s, 6 H, *p*-CH_3), 2.51 (sep, $^3J_{HH}$ = 6.8 Hz, 2 H, *o*-$CH(CH_3)_2$), 2.88 (sep, $^3J_{HH}$ = 6.8 Hz, 1 H, *p*-$CH(CH_3)_2$), 6.97–7.01 (m, 7 H, various aryl-H), 6.89 (s, 4 H, *m*-Mes), 7.11 (s, 2 H, *m*-Trip). **^{13}C NMR** (62.9 MHz): δ = 21.1 (*o*-CH_3), 21.2 (*p*-CH_3), 24.2, 24.5, 24.7 (*o*/*p*-$CH(CH_3)_2$), 30.6 (*o*-$CH(CH_3)_2$), 34.5 (*p*-$CH(CH_3)_2$), 119.0, 121.8, 122.9, 123.4, 126.3, 128.3, 130.0, 131.4 (aromatic *C*-H), 129.7, 134.7, 135.5, 136.4, 137.9, 143.6, 144.6, 147.5, 150.7 (aromatic *C*); one aromatic C signal could not be observed. **IR** (Nujol) 1612 s, 1592 ms, 1568 s, 1313 vs, 1288 s, 1207 s, 1189 s, 1166 vs. br, 1092 s, 1069 ms, 1054 ms, 1003 m, 978 m, 946 w, 937

Table 2. Selected Crystallographic Data for Compounds **2a**, **2b**, and **3a**[a].

	2a	**3a**	**2b**
Formula	$C_{39}H_{40}ClHgN_3$	$C_{39}H_{40}BrHgN_3$	$C_{45}H_{52}ClHgN_3$
Formula weight	786.78	831.24	870.94
Color, habit	pale yellow, prism	pale yellow, prism	yellow, prism
Crystal size/mm	0.35 × 0.25 × 0.20	0.30 × 0.25 × 0.15	0.38 × 0.35 × 0.30
Crystal system	triclinic	triclinic	triclinic
Space group	$P\bar{1}$	$P\bar{1}$	$P\bar{1}$
a /Å	8.2637(18)	8.384(6)	12.401(3)
b /Å	11.088(3)	11.031(8)	12.623(3)
c /Å	18.861(5)	18.944(9)	15.146(3)
α /°	82.56(2)	82.81(5)	79.997(15)
β /°	89.950(19)	89.32(5)	84.084(15)
γ /°	88.89(2)	88.16(5)	61.170(16)
V /Å^3	1713.3(7)	1737(2)	2045.0(8)
Z	2	2	2
d_{calc} /g·cm^{-3}	1.525	1.589	1.414
μ /cm^{-1}	46.00	56.10	3.862
2θ range/°	4.0–56.0	3.7–50.4	3.7–54.0
Collected data	8499	6414	9346
Unique data (R_{int})	8035 (0.019)	5975 (0.056)	8923 (0.049)
Data with $I > 2\sigma(I)$ (N_o)	7425	4263	7523
No. of parameters (N_p)	421	398	467
$R1$ ($I > 2\sigma(I)$)[b]	0.033	0.079	0.043
$wR2$ (all data)[c]	0.086	0.211	0.101
GOF [d]	1.159	1.256	1.174
Resd. dens./e·Å^{-3}	1.61 and –1.92	3.32 and –3.34	1.99 / –1.04

a) All data were collected at 173 K using Mo-K_α (λ = 0.71073 Å) radiation. b) $R1 = \Sigma(\|F_o\| - \|F_c\|)/\Sigma(\|F_o\|$. c) $wR2 = \{\Sigma[w(F_o^2-F_c^2)^2]/\Sigma[w(F_o^2)^2]\}^{1/2}$. d) GOF = $\{\Sigma[w(F_o^2-F_c^2)^2]/(N_o-N_p)$.

ms, 879 s, 864 m, 848 vs, 805 s, 788 s, 779 m, 764 vs, 755 vs. br, 740 s, 723 s, 692 m, 656 ms, 602 w, 594 m, 491 w cm^{-1}.

Redox Transmetallation Reactions

Iodo-{[[N'-2-(2',4',6'-triisopropyl)biphenyl]-(N'''-2,4,6,2'',4'',6''-hexamethyl-1,1':3',1''-terphen-2'-yl)]triazenido-N',N'''}-(tetrahydrofuran-O)-magnesium (5b): A solution of **4b** (0.63 g, 1 mmol) in tetrahydrofuran (40 mL) was added to an excess of magnesium turnings and the mixture was stirred for 3 d at ambient temperature. The volatile materials were removed under reduced pressure and the remaining solid was extracted with *n*-heptane (40 mL). Solid byproducts were separated by centrifugation and the filtrate was concentrated to incipient crystallization. Storage at ambient temperature for several days afforded **5b** as deep yellow crystals. Yield: 0.58 g (0.68 mmol, 68 %); Mp: 70–120 °C (dec.). $C_{49}H_{60}IMgN_3O$ (858.2): C 69.19 (calcd. 68.58); H 7.02 (7.05); N 4.87 (4.90) %. **^{1}H NMR** (400.1 MHz): δ = 1.02, 1.15 1.29 (3 × d, $^3J_{HH}$ = 6.8 Hz, 3 × 6 H, *o*- + *p*-CH(*CH*$_3$)$_2$), 1.11 (m, 4 H, OCH$_2$*CH*$_2$); 2.15 (s, 12 H, *o*-CH$_3$), 2.21 (s, 6 H, *p*-CH$_3$), 2.60 (sep, $^3J_{HH}$ = 6.8 Hz, 2 H, *o*-*CH*(CH$_3$)$_2$), 2.84 (sep, $^3J_{HH}$ = 6.8 Hz, 1 H, *p*-*CH*(CH$_3$)$_2$), 3.06 (m, 4 H, O*CH*$_2$CH$_2$), 6.79–7.12 (m, 13 H, various aryl-H). **^{13}C NMR** (100.6 MHz): δ = 21.2, 21.6 (*o*/*p*-CH$_3$), 24.3, 24.3, 25.0 (*o*/*p*-CH(*CH*$_3$)$_2$), 25.3 (OCH$_2$*CH*$_2$), 30.4 (*o*-*C*H(CH$_3$)$_2$), 34.8 (*p*-*C*H(CH$_3$)$_2$), 70.1(O*C*H$_2$CH$_2$), 113.8, 121.2, 121.5, 125.0, 128.9, 129.7, 130.5, (aryl CH), 123.8, 132.0, 133.9, 136.0, 139.6, 139.6, 143.9, 147.3, 148.3, 149.5 (aryl C); one aromatic CH signal could not be observed.

Bis[μ-chloro-{[[N'-2-(2',4',6'-triisopropyl)biphenyl]-(N'''-2,4,6,2'',4'',6''-hexamethyl-1,1':3',1''-terphen-2'-yl)]triazenido-N',N'''}(tetrahydrofuran-O)-ytterbium] (6b): A solution of **2b** (1.01 g, 1.15 mmol) in tetrahydrofuran (40 mL) was added to an excess of ytterbium chips (0.71 g, 4.10 mmol) and the stirred mixture was heated for 2 min to 50 °C. A color change to brown was observed and stirring was continued for 20 h at ambient temperature. The volatile materials were removed under reduced pressure and the remaining solid was extracted with an *n*-heptane/toluene 2:1 solvent mixture (60 mL). Solid byproducts were separated by centrifugation and the filtrate was concentrated to incipient crystallization. Storage at –10 °C for 3 days afforded **6b**·(toluene)$_2$ as dark red crystals. Yield: 0.98 g (0.89 mmol, 77 %); Mp: 68–180 °C (dec.); Because of paramagnetic impurities no NMR spectra could be obtained. For the following characterization the co-crystallized toluene was removed in vacuum. $C_{49}H_{60}ClN_3OYb$ (915.5): C 64.36 (calcd. 64.28); H 6.73 (6.61); N 4.51 (4.59) %. **IR** (Nujol) 1604 s, 1581 ms, 1568 s, 1432 vs, 1360 s, 1310 s, 1291 vs, 1255 vs. br, 1232 vs. br, 1218 vs, 1178 s, 1106 ms, 1076 ms, 1056 m, 1031 vs. br, 1004 s, 953 m, 936 ms, 920 w, 908 w, 876 vs, 847 vs, 800 ms, 788 m, 781 ms, 769 s, 752 vs, 739 s, 727 vs, 694 s, 678 ms, 653 ms, 622 w, 600 w, 586 m, 576 w, 551 w, 523 m, 506 m, 464 ms, 409 w cm^{-1}. **EI-MS** (70eV, 520 K): *m*/*z* (%) 195.0 (12.4) [MesC$_6$H$_4^+$], 312.1 (100) [2,6-Mes$_2$C$_6$H$_3$–H$^+$], 341.1 (6.2) [2,6-Mes$_2$C$_6$H$_3$N$_2^+$], 607.3 (44.1) [(2,6-Mes$_2$C$_6$H$_3$)(C$_6$H$_4$Trip)NH$^+$], 916.4 (14.5) [M$^+$].

X-ray Crystallographic Studies

X-ray-quality crystals were obtained as described in the Experimental Section. Crystals were removed from Schlenk tubes and immediately covered with a layer of viscous hydrocarbon oil (Paratone N, Exxon). A suitable crystal was selected, attached to a glass fiber, and instantly placed in a low-temperature N$_2$-stream [27a]. All data were collected at 173 K using either a Siemens P4 (**3a**) or a rebuilt Syntex *P*2$_1$/*S*iemens P3 (**2a**, **2b**, **4b**–**6b**) diffractometer. Selected data collection parameters and other crystallographic data are summarized in Table 2 and Table 3.

Table 3. Selected Crystallographic Data for Compounds **4b**, **5b**, and **6b**[a)].

	4b	**5b**	$(\mathbf{6b})_2\cdot(C_7H_8)_3$
Formula	$C_{45}H_{52}HgIN_3$	$C_{49}H_{60}IMgN_3O$	$C_{119}H_{144}Cl_2N_6O_2Yb_2$
Formula weight	962.39	858.21	2107.38
Color, habit	yellow, prism	yellow, prism	dark red, prism
Crystal size/mm	0.35 × 0.25 × 0.25	0.50 × 0.30 × 0.15	0.55 × 0.25 × 0.15
Crystal system	monoclinic	monoclinic	triclinic
Space group	$P2_1/c$	$P2_1/n$	P1
a /Å	8.8388(11)	9.6393(18)	14.079(3)
b /Å	21.681(3)	39.797(6)	15.807(4)
c /Å	21.817(2)	12.926(2)	25.661(7)
α /°			77.000(19)
β /°	93.059(10)	110.65(2)	81.487(19)
γ /°			82.425(19)
V /Å^3	4174.9(9)	4640.0(13)	5474(2)
Z	4	4	2
$d_{calc.}$ /g•cm^{-3}	1.531	1.229	1.278
μ /cm^{-1}	44.59	7.40	17.97
2θ range /deg	3.7–54.0	3.5–52.0	3.2–54.0
Collected data	9692	9826	24790
Unique data (R_{int})	9103 (0.037)	9100 (0.029)	23799 (0.046)
Data with $I > 2\sigma(I)$ (N_o)	6670	5989	16108
No. of parameters (N_p)	471	513	1168
R1 ($I>2\sigma(I)$)[b)]	0.050	0.050	0.081
wR2 (all data)[c)]	0.106	0.102	0.190
GOF [d)]	1.214	1.359	1.450
Resd. dens./e·Å^{-3}	1.31 / –1.44	0.54 / –0.62	3.11 / –1.13

a) All data were collected at 173 K using Mo-K_α (λ = 0.71073 Å) radiation. b) $R1 = \Sigma(\|F_o| - |F_c\|)/\Sigma(|F_o|$. c) $wR2 = \{\Sigma[w(F_o^2-F_c^2)^2]/\Sigma[w(F_o^2)^2]\}^{1/2}$. d) GOF = $\{\Sigma[w(F_o^2-F_c^2)^2]/(N_o-N_p)$.

Calculations were carried out with the SHELXTL PC 5.03 [27b] and SHELXL-97 [27c], program system installed on local personal computers. The phase problem was solved by direct methods and the structures were refined on F_o^2 by full-matrix least-squares refinement. Absorption corrections were applied by using semiempirical ψ-scans. Anisotropic thermal parameters were refined for all non-hydrogen atoms, except some carbon atoms of disordered THF molecules. The hydrogen atoms were positioned at distances of 1.00 (CH), 0.99 (CH_2) and 0.98 Å (CH_3) and refined in a riding model approximation, including free rotation for methyl groups and variable isotropic displacement parameters. In **3a** and **4b**, the mercury atoms are disordered and were refined with split positions. The major occupancy (**3a**: 0.961, **4b**: 0.983) corresponds to a η^1-N3 coordination mode whereas the minor occupancy (**3a**: 0.039, **4b**: 0.017) is in accordance with a η^1-N1 coordination. In **2a**, the mercury and chlorine atoms were refined with split positions (η^1-N3: 0.974, η^1-N1: 0.026). In **6b**, carbon atoms of two disordered THF molecules were refined with split positions and corresponding site occupation factors of 0.50 (C3/C3a and C7/C7a) together with SADI restraints for some C–C distances. Four additional toluene molecules were located in solvent accessible cavities of the structure. Because one of them was heavily disordered, its contribution was eliminated from the reflection data using the BYPASS method [27d] as implemented in the SQUEEZE routine of the PLATON98 [27e] package. For the other three toluene molecules the geometry of the arene rings was constrained to regular hexagons. Final R values are listed in Table 2 and Table 3. Important bond lengths and angles are given in Table 1, Figure 3, and Figure 4. Crystallographic data (excluding structure factors) for the structures reported in this paper have been deposited with the Cambridge Crystallographic Data Centre as supplementary publication no. CCDC-750294 (**2a**), CCDC-750295 (**3a**), CCDC-750296 (**2b**), CCDC-750297 (**4b**), CCDC-750298 (**5b**), and CCDC-750299 (**6b**). Copies of the data can be obtained free of charge on application to CCDC, 12 Union Road, Cambridge CB2 1EZ, UK (Fax: +44-1223-336-033; E-Mail:deposit@chemcrys.cam.ac.uk.

Supporting Information (see footnote on the first page of this article): Molecular structures of **2a**, **2b**, **3a**, **4b**, **5b**, and **6b** showing the full numbering scheme. Molecular plots showing the disorder in **2a**, **3a**, and **4b**.

Acknowledgement

Support of this work by the *Deutsche Forschungsgemeinschaft* within the priority program SPP 1166 (Lanthanoid-spezifische Funktionalitäten in Molekül und Material) is gratefully acknowledged.

References

[1] V. C. Gibson, S. K. Spitzmesser, *Chem. Rev.* **2003**, *103*, 283.
[2] L. Bourget-Merle, M. F. Lappert, J. R. Severn, *Chem. Rev.* **2002**, *102*, 3031.
[3] J. Barker, M. Kilner, *Coord. Chem. Rev.* **1994**, *133*, 219.
[4] a) D. D. Moore, S. D. Robinson, *Adv. Inorg. Chem. Radiochem.* **1986**, *30*, 1; b) K. Vrieze, G. van Koten, in: *Comprehensive Coordination Chemistry* (Ed.: G. Wilkinson), Pergamon Press, Oxford, **1987**, Vol. 2, p. 189.
[5] S.-O. Hauber, F. Lissner, G. B. Deacon, M. Niemeyer, *Angew. Chem. Int. Ed.* **2005**, *44*, 5871.
[6] H. S. Lee, M. Niemeyer, *Inorg. Chem.* **2006**, *45*, 6126.
[7] S. Balireddi, M. Niemeyer, *Acta Crystallogr., Sect. E* **2007**, *63*, o3525.
[8] a) N. Nimitsiriwat, V. C. Gibson, E. L. Marshall, P. Takolpuckdee, A. K. Tomov, A. J. P. White, D. J. Williams, M. R. J. Elsegood, S. H. Dale, *Inorg. Chem.* **2007**, *46*, 9988; b) A. G. M. Barrett, M. R. Crimmin, M. S. Hill, P. B. Hitchcock, G. Kociok-Köhn, P. A. Procopiou, *Inorg. Chem.* **2008**, *47*, 7366; c) S. G. Alexander, M. L. Cole, C. M. Forsyth, S. K. Furfari, K. Konstas, *Dalton Trans.* **2009**, 2326.
[9] S.-O. Hauber, M. Niemeyer, *Inorg. Chem.* **2005**, *44*, 8644.

[10] H. S. Lee, S.-O. Hauber, D. Vinduš, M. Niemeyer, *Inorg. Chem.* **2008**, *47*, 4401.

[11] a) M. Hörner, G. M. de Oliveira, J. S. Bonini, H. Fenner, *J. Organomet. Chem.* **2006**, *691*, 655; b) M. Hörner, G. M. de Oliveira, V. F. Giglio, L. do Canto Visentin, F. Broch, J. Beck, *Inorg. Chim. Acta* **2006**, *359*, 2309; c) M. Hörner, G. M. de Oliveira, M. Bohneberger Behm, H. Fenner, *Z. Anorg. Allg. Chem.* **2006**, *632*, 615.

[12] a) M. Hörner, G. M. de Oliveira, J. A. Naue, J. Daniels, J. Beck, *J. Organomet. Chem.* **2006**, *691*, 1051; b) M. Hörner, G. M. de Oliveira, E. G. Koehler, L. do Canto Visentin, *J. Organomet. Chem.* **2006**, *691*, 1311; c) M. Hörner, G. M. de Oliveira, L. do Canto Visentin, R. S. Cezar, *Inorg. Chim. Acta* **2006**, *359*, 4667.

[13] M. Hörner, A. J. Bortoluzzi, J. Beck, M. Serafin, *Z. Anorg. Allg. Chem.* **2002**, *628*, 1104.

[14] a) P. I. van Vliet, M. Kokkes, G. van Koten, K. Vrieze, *J. Organomet. Chem.* **1980**, *187*, 413; b) P. E. Jaitner, P. Peringer, G. Huttner, L. Zsolnai, *Transition Met. Chem.* **1981**, *6*, 86.

[15] M. R. Melardi, M. K. Rofouei, J. Massomi, *Anal. Sci.: X-ray Struct. Anal. Online* **2007**, *23*, x67.

[16] a) M. Tsunoda, F. P. Gabbaï, *J. Am. Chem. Soc.* **2000**, *122*, 8335; b) M. R. Haneline, M. Tsunoda, F. P. Gabbaï, *J. Am. Chem. Soc.* **2002**, *124*, 3737; c) M. R. Haneline, J. B. King, F. P. Gabbaï, *Dalton Trans.* **2003**, 2686; d) M. A. Omary, R. M. Kassab, M. R. Haneline, O. Elbjeirami, F. P. Gabbaï, *Inorg. Chem.* **2003**, *42*, 2176; e) T. J. Thomas, V. I. Bakhmutov, F. P. Gabbaï, *Angew. Chem. Int. Ed.* **2006**, *45*, 7030; f) I. A. Tikhonova, K. I. Tugashov, F. M. Dolgushin, A. A. Yakovenko, B. N. Strunin, P. V. Petrovskii, G. G. Furin, V. B. Shur, *Inorg. Chim. Acta* **2006**, *359*, 2728; g) T. J. Thomas, C. N. Burress, L. Pandey, F. P. Gabbaï, *Dalton Trans.* **2006**, 4654; h) T. J. Taylor, C. N. Burress, F. P. Gabbaï, *Organometallics* **2007**, *26*, 5252.

[17] a) C. N. Burress, M. I. Bodine, O. Elbjeirami, J. H. Reibenspies, M. A. Omary, F. P. Gabbaï, *Inorg. Chem.* **2007**, *46*, 1388; b) G. B. Deacon, C. M. Forsyth, P. C. Junk, T. J. Ness, E. Izgorodina, J. Baldamus, G. Meyer, I. Pantenburg, J. Hitzbleck, K. Ruhlandt-Senge, *Eur. J. Inorg. Chem.* **2008**, 4770.

[18] a) P. B. Hitchcock, *Acta Crystallogr., Sect. B* **1979**, *35*, 746; b) M. Niemeyer, P. P. Power, *Organometallics* **1997**, *16*, 3258.

[19] a) W. Lau, J. C. Huffman, J. K. Kochi, *J. Am. Chem. Soc.* **1982**, *104*, 5515; b) A. S. Borovik, S. G. Bott, A. R. Barron, *J. Am. Chem. Soc.* **2001**, *123*, 11219.

[20] S. Westhusin, P. Gantzel, P. J. Walsh, *Inorg. Chem.* **1998**, *37*, 5956.

[21] J. Prust, K. Most, I. Müller, E. Alexopoulos, A. Stasch, I. Usón, H. W. Roesky, *Z. Anorg. Allg. Chem.* **2001**, *627*, 2032.

[22] a) A. R. Sadique, M. J. Heeg, C. H. Winter, *Inorg. Chem.* **2001**, *40*, 6349; b) J. A. R. Schmidt, J. Arnold, *J. Chem. Soc., Dalton Trans.* **2002**, 2890; c) A. Xia, H. M. El-Kaderi, M. J. Heeg, C. H. Winter, *J. Organomet. Chem.* **2003**, *682*, 224; d) R. T. Boeré, M. L. Cole, P. C. Junk, *New J. Chem.* **2005**, *29*, 128.

[23] D. Heitmann, C. Jones, P. C. Junk, K.-A. Lippert, A. Stasch, *Dalton Trans.* **2007**, 187.

[24] a) A. G. Avent, P. B. Hitchcock, A. V. Khvostov, M. F. Lappert, A. V. Protchenko, *Dalton Trans.* **2003**, 1070; b) S. Harder, *Angew. Chem. Int. Ed.* **2004**, *43*, 2714.

[25] L. Zhou, J. Wang, Y. Zhang, Y. Yao, Q. Shen, *Inorg. Chem.* **2007**, *46*, 5763.

[26] a) M. Niemeyer, *Z. Anorg. Allg. Chem.* **2002**, *628*, 647; b) S. A. A. Shah, R. Murugavel, H. W. Roesky, H.-G. Schmidt, *Bull. Pol. Acad. Sci., Chem.* **1998**, *46*, 157.

[27] a) H. Hope, *Prog. Inorg. Chem.* **1994**, *41*, 1; b) *SHELXTL PC 5.03*, Siemens Analytical X-ray Instruments Inc.: Madison, WI, **1994**; c) G. M. Sheldrick, *SHELXL-97*, Program for Crystal Structure Solution and Refinement, Universität Göttingen, **1997**; d) A. L. Spek, *Acta Crystallogr., Sect. A* **1990**, *46*, 194; e) A. L. Spek, *PLATON-98*; Utrecht University: Utrecht, The Netherlands, **1998**.

Received: October 9, 2009